Multitemporal RADARSAT-2 Polarimetric SAR Data for Urban Land Cover Classification Using Support Vector Machine

Xin NIU[1], and Yifang BAN
Division of Geoinformatics,Department of Urban Planning and Environment, Royal Institute of Technology – KTH

Abstract. This research investigates the various RADARSAT-2 polarimetric SAR features for urban land cover classification using object-based method combining with support vector machine (SVM) and ruled-based approach. Six-dates of RADARSAT-2 fine-beam polarimetric SAR data were acquired in the rural-urban fringe of Greater Toronto Area during June to September, 2008. The major landuse/land-cover classes were high-density built-up areas, low-density built-up areas, roads, forests, parks, golf courses, water and several types of agricultural crops. The polarimetric SAR features examined are the parameters from Pauli, Freeman and Cloude-Pottier decompositions as well as the elements from coherence matrix and the intensities and their logarithm form of each channel. For urban land cover classification, SVM is combined with rule-based method for the object-based classification. The image objects containing the multitemporal polarimetric features were classified using the SVM classifier first. The SVM classification results were further refined using a rule-based approach. Rules were built to recognize specific classes defined by the shape features and the spatial relationships within the context. In terms of the effectiveness of different SAR ploarimtric parameters, the results indicated that the processed Pauli feature set could produce best classification result while the use of all the polarimetric features did not produce the best classification result. The raw Pauli parameters could generate similar result as all T elements. The logarithm parameters such as log intensity and processed Pauli parameters perform better than the intensity and raw Pauli respectively. The proposed object-based classification using SVM and rule-based approach yielded higher classification accuracies than the object-based classification using nearest neighbor classifier.

Keywords. Polarimetric SAR, multitemporal, landuse/land-cover, SVM, object-based analysis

Introduction

Urbanization is considered one of the main causes for the global environmental change. Therefore, regular update of urban landuse/land-cover maps is of critical importance for sustainable planning and environment protection [1]. As one of the most advanced Synthetic Aperture Radar (SAR) satellite, RADARSAT-2 offers the opportunity for mapping earth surface features with high resolution in multi-polarization. Its all-weather capability and its ability to acquired unique information in high-resolution makes RADARSAT-2 a very attractive data source for monitoring urban expansions.

To explore and analyze the polarimetric information from the observed land cover classes, various decomposition methods are compared. The parameters generated from those decompositions like the Cloude-Pottier decomposition [5] and Freeman decomposition [6] are well applied in the previous polarimetric SAR landuse /land-cover studies. However, the utilizations of the parameters are less compared especially in the urban area.

[1] Xin Niu: Drottning Kristinas väg 30, 100 44 Stockholm, Sweden; E-mail:xin.niu@abe.kth.se

Studies on improving the classification accuracy lead to the introducing of the theoretically superior machine learning classifier, Support Vector Machine (SVM) into both the pixel-based and object-based analysis [2,3]. In recent years, SVM has been gaining increasing popularity in the remote sensing field comparing with the other traditional classifiers [4]. However, the efficiency of using SVM on the multitemporal polarimetric SAR objects by combining the rule-based methods for the urban area are less reported.

Therefore, in this paper, we focus on the comparison of the classification accuracy applying various polarimetric SAR parameters using object-based analysis through SVM.

1. Study area and data description

The study area is located in the northern urban-rural fringe of the Greater Toronto Area (GTA), Ontario, Canada, where urban area is sprawling towards the Oak Ridges Moraine, an environmentally sensitive area. Significant environmental changes has undergone due to rapid urban expansion. The main landuse/land-cover types are high-density built-up areas, low-density built-up areas, industry areas, constructing areas, wide roads, streets, parks, forests, golf courses, water, pasture and several kinds of crops.

Six-date RADARSAT-2 fine-beam Polarimetric SAR data were acquired over the study area during summer 2008. The data are single look complex products, fully polarimetric including HH, HV, VH and VV polarizations with fine resolution at 4.7 and 5.1 metres in the range and azimuth directions respectively. The centre frequency of this beam mode is 5.4 GHz, i.e., C-band. The detailed descriptions of these images are given in Table 1.

Table 1. RADARSAT-2 Fine Quad-Pol SAR Imagery

Data	Orbit	Incident angle	Data	Orbit	Incident angle
Jun. 11 2008	Ascending	40.18~ 41.59	Aug. 06 2008	Descending	40.20~ 41.61
Jun. 19 2008	Descending	40.22~ 41.62	Aug. 22 2008	Ascending	40.17~ 41.59
Jul. 05 2008	Ascending	40.18~ 41.60	Sep. 15 2008	Ascending	40.17~ 41.59

The acquisition dates of the SAR data span from June to September in 2008. Most of the crops experienced from the growing stage to harvest within the time, while the urban structures exhibit relatively stable character except some progress in the construction areas. The ascending and descending orbits provide two different views of the observed objects, thus provide the complement information. All the data within the same orbit are collected in similar incident angles, therefore relatively constant data value could be recorded for the temporally stable objects such as built up from different dates, which is beneficial for the multitemporal classification.

2. Method

The proposed object-based multitemporal classification scheme is illustrated in Figure 1. After the preprocessing of the raw data, multi-scale segmentations are performed on the corresponding data sets as the basis for the object-analysis. All the other landuse/land-cover types, except wide roads, streets and parks, are classified using SVM. The extraction of wide roads is performed using rule-based approach. Then, the SVM classification results and the road maps are fused together. Finally, parks and streets are identified from the fused map through the rules developed. The segmentation and the rules for object-based analysis are implemented in the eCognition software [7].

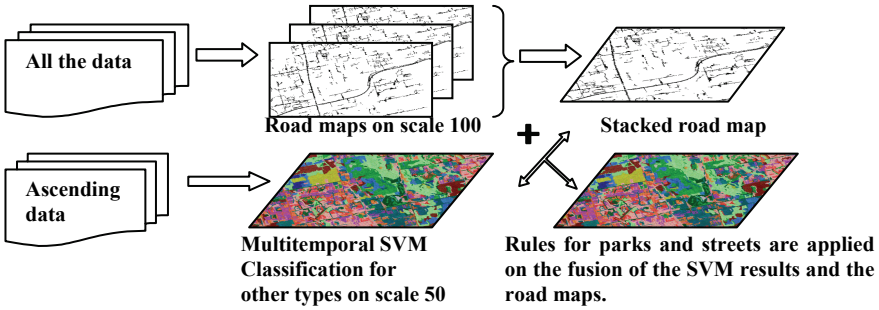

Figure 1. Multitemporal classification scheme.

2.1. Preprocessing

2.1.1. Ortho-rectification and co-registration

The six-date raw data were orthorectified to the National Topographic Database (NTDB) vector map using the RADARSAT-2 orbital model using the DEM with resolution of 30m. Hence, the relief displacements caused by terrain and the two opposite look directions could be removed. Consequently, the roads and streets in all the images are matched well.

2.1.2. Comparison feature sets selection

The behaviours of various polarimetric SAR parameters used in the previous studies for the object-based urban analysis are the concerns of this study. The candidate feature sets selected are listed in table 2. The 3x3 hermitian coherency matrix for SAR data on each date are extracted first. For the reciprocal target matrix, under the mono-static assumption in which the Sinclair scattering matrix to be symmetrical, i.e., $HV=VH$, the coherency matrix $\langle T \rangle$ could be constructed through the Pauli target vector like [6]:

$$\underline{k} = \frac{1}{\sqrt{2}}\left[HH+VV \quad HH-VV \quad 2HV\right]^T \tag{1}$$

$$\langle \mathrm{T} \rangle = \underline{k} \cdot \underline{k}^{*T} \tag{2}$$

The Pauli parameters: $|HH+VV|^2$, $|HH-VV|^2$ and $|HV|^2$ were directly obtained as the diagonal elements of the coherency matrix $\langle T \rangle$. Freeman and Cloude-Pottier decompositions are carried based on the coherency matrix $\langle T \rangle$ as well. The Double-bounce (D), Odd-bounce (O), and Volume (V) parameters of the Freeman decomposition represent the scattering mechanisms of the observed objects [6]. The Entropy (H), Anisotropy (A) and Alpha (a) parameters from Cloude-Pottier decomposition reveal the polarimetric properties of the backscatterings [5]. The elements of the 3x3 hermitian coherency matrices $\langle T \rangle$ that contain the full polarimetric information are also selected as a classification feature set for comparison.

It is reported by Rignot [8] that the usage of the logarithm of the parameters has the following advantages: Fist, the robustness of the clustering center selection which is interfered by the speckles could be improved as the noise has the additive statistic characteristics in the log-domain. Second, the unbalance data driven force in clustering caused by the difference of orders of magnitude between the cross-polarization and co-polarization scattering powers could be reduced.

Therefore, the effects of using the logarithm parameters were investigated. Besides the scattering intensities for HH, HV and VV polarizations, the logarithm of the intensities and Pauli parameters are selected for comparison. In addition, previous research indicated that it is reasonable to

compress the original noisy images to achieve better classification results [9]. Thus the logarithm Pauli parameters were compressed into 8-bit as another feature set through linear scaling.

Table 2. Selected feature sets for comparison

Feature Set	Elements	Feature Set	Elements
Intensity	$\|HH\|^2$, $\|HV\|^2$, $\|VV\|^2$	Processed Pauli	$(\text{Log(Pauli)})_{8\text{-bit}}$
Logarithm Intensity	Log (Intensity)	Freeman	D, O, V
Coherency Matrix	$<T>$	Cloude-Pottier	H, A, a
Pauli	T_{11}, T_{22}, T_{33}		

2.1.3. Segmentation

The segmentations of the objects are performed on the compressed 8-bit Pauli images filtered by the refined Lee filter [10] with window size of 7×7. The superiority of using the compressed 8-bit data rather than the raw 16-bit data for the segmentation has been reported by Hu & Ban [3]. Multi-resolution segmentation algorithm introduced by Baatz and Schape [11] is chosen for this segmentation task.

For the wide roads mapping task, the segment scale is set as 100, and each date data has its own segmentation. For multitemporal SVM classification of the other classes, the segment scale is set as 50, and only one segmentation result is obtained over the stacked processed Pauli images of the ascending groups.

2.2. Road extraction

The wide roads are extracted mainly according to the shape features of the objects. The longer and moderate wide segments with fewer curves are defined as wide roads. Thereby, the rules are specified considering the ratio of the length to the width, the width range of the object. Besides, the flat road usually has lower backscatter, especially in the cross-polarization channel *HV*. According to those rules, one road map is extracted for each date. Final road map is generated to record the overlap ratio of the road segments of the stacked road maps from each date, where the high ratio predicates the high possibility of the road segments.

2.3. Object-based SVM classification of multitemporal SAR data

The SVM is an advanced conception of binary classifier. Through mapping the input vectors into the high dimension space, SVM searches for the optimal hyper plane to separate the two classes. For mapping the high dimension space, the RBF kernel which is the most popular one is used in our study:

$$k(x_i, x_j) = \exp(-\gamma \| x_i - x_j \|^2), \gamma > 0 \tag{3}$$

Tow parameters are required to be determined in the SVM model using this kernel: The penalty value C and γ. Best parameters are picked up by a cross-validation process on the defined searching grids. For detailed description one could refer to [12]. For multi class classification, one-against-one approach [13] implemented in LIBSVM [14] is applied. Since there is no assumption of the statistic model for the distribution of the data to be classified, SVM is appropriate for classification of multitemporal or multisensor data.

In our study, high-density built-up areas, low-density built-up areas, industrial areas, constructing areas, forests, golf courses, water, pasture and several types of crops are classified directly by the multitemporal SVM classification. Only the ascending data are selected for the SVM classification. For each feature set, consistent features are calculated for each date. Those features of one specific feature set from four-date data are stacked as multitemporal feature layers. In the object-

based SVM classification, the actual input vector comprises the Means and Standard deviations of the pixel values within the object on the above multitemporal feature layers. The other components are Brightness and Max diff. Brightness is defined as the mean value of the mean values of an image object in the multitemproal feature layers while the Max.diff is calculated as the subtraction of the maximum and the minimum mean values in the multitemproal feature layers, subsequently normalized by the Brightness.

2.4. Fusion of the road map and the SVM classification

Various rules are developed to fuse the road map and the SVM classification result together. The final road map, for example, include a large number of golf and street segments since they are similar in terms of both scattering and shape characteristics. However, most of the golf courses that were wrongly mapped on the road map have relatively lower road overlap ratio. Thus, if the roads cover the golf objects from the SVM classification, those objects will be mapped as roads only when they have higher road overlap ratio. For the other SVM classified objects, a relatively lower overlap ratio could be accepted as the mapping criterion into the road type. And the streets will classified on the road fused map by the shape character as narrow and winding segments enclosed in the urban area. If crops and pastures are surrounded by the buildups, then they will be assigned as parks. At last, the final mapping result is improved by filtering away the tiny isolated objects within the area dominated by the other classes.

3. Result and discussion

The comparison of the SVM efficiency on various polarimetric parameters through object-based approach is conducted in three respects. These comparisons include:

1. the predicted fairness of the best selected features for various input feature number among different feature sets.
2. final results of using all the features between the feature sets.
3. results of using SVM and Nearest Neighbor (NN) classifier.

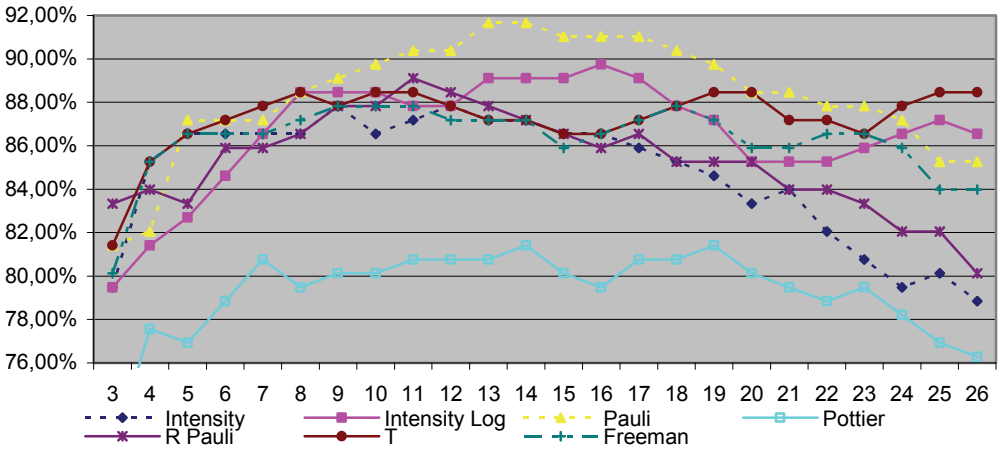

Figure 2. Predication comparison of step forward selected features. X-axis scale are the input numbers; Y-axis scale gives the predicated accuracy.

3.1. Step forward best features performance comparison

This proposed comparison scheme stems from the optimization of features selection for specified input number [15]. Although the objects for experiment are limited in a few selected samples, the

classification capacity and accuracy trend of different parameter sets could be roughly revealed by considering the influence from the numbers of input features. At each step, one feature, which contributes the best predicted overall accuracy working with the previously selected features, will be added to the best feature group. The overall accuracy is predicted from the cross-validation. The cross-validation process divides the samples into several groups, and then each group, one time, will be used for validation for the predicted results from the other groups. The overall accuracy is constituted by those validations. Figure 2 shows the comparison result between our feature sets, from which the following observations could be made. The use of all the features did not produce the best classification results. The processed Pauli feature set could generate best result, while the Cloude-Pottier parameter set yielded the lowest accuracy given any input number. The raw Pauli parameters (the diagonal elements of the coherence matrix T) could provide approximately as good result as all T elements. The logarithm parameters such as log Intensity and Processed Pauli parameters perform better than the Intensity and Raw Pauli respectively.

3.2. Comparison of using different feature sets and comparison between SVM and NN

The final classification results of using all the features within each feature set by our proposed classification scheme are given in Table 3. In urban classes, the construction areas are well classified while the industrial areas have some confusion with the high-density built-up areas. The low-density built-up areas are well distinguished from the forest, which is mainly attributed to the object analysis scheme. The producer accuracy (Pro) of park is not quite satisfactory, this mainly due to its confusion with the pasture class. Golf courses, water and pastures could be successfully differentiated by their scattering properties only. The various crops are well classified on account of their multitemporal attributes.

By comparison of the different feature set, similar conclusion to the step forward comparison could be made. The processed Pauli parameters could produce the best classification results. The use of raw pauli parameters only could generate similar results as that of using all the elements of coherence matrix T. The logarithm parameters perform better than the normal ones. The examples of that are given between the sets of Intensity and Intensity Log, and processed Pauli and raw Pauli parameters. Freeman decomposition parameters could bring nice classification results while the results from Cloude-Pottier parameters are poorer than expected, even not as well as that of using only the intensity parameters. The main reason maybe due to that the Cloude-Pottier parameters do not explore all the polarimetric information.

The results of replacing the SVM classifier with the NN classifier applied on the optimal processed Pauli feature set are also reported in table 3, from which the distinct superiority of using SVM classifier compared to the NN are observed.

4. CONCLUSIONS

RADARSAT-2 fine-beam polarimetric SAR data were evaluated for land-cover mapping in the rural-urban fringe of the Greater Toronto Area. The multi-temporal classification method applied on the six-date data could generate higher classification result with overall accuracy of 86.79% and Kappa coefficient 0.85 for the major 14 land-cover classes by using processed Pauli parameters. In the object-based analysis, the SVM classifier shows superiority to the NN classifier. It is also demonstrated that the logarithm parameters could bring better results than the normal ones. And classification using only raw Pauli parameters could produce similar results as that of using all the elements of the coherency matrix.

Table 3. Classification comparisons of using different parameter sets and comparison between SVM and NN.

classes	Pauli		Raw Pauli		T		Freeman	
	Pro	User	Pro	User	Pro	User	Pro	User
Constructing	96.88	90.75	87.31	92.77	81.2	93.23	99.76	96.75
Industry	72.75	90.77	61.25	82.67	68.62	82.54	77.65	87.64
High Density	79.77	74.59	75.12	70.15	73.45	76.54	80.18	83.94
Low Density	74.9	73.07	70.35	62.04	69.06	56.49	77.19	61.01
Park	55.87	88.61	32.51	88.47	46.13	87.23	34.39	79.54
Pasture	91.47	77.91	91.36	67.67	94.76	68.42	96.6	72.69
Golf Course	84.52	82.31	76.9	68.33	71.49	79.73	76.94	73.77
Street	61.85	47.26	61.92	47.54	60.99	47.14	61.85	47.6
Wide Road	67.78	40.98	59.58	36.78	60.45	37.58	44.41	31.74
Crop 1	99.65	93.57	92.37	91.15	97.46	92.08	96.94	98.15
Crop 2	89.03	94.41	83.38	94.11	75.14	85.04	90.19	94.28
Crop 3	90.99	85.92	94.85	81.34	79.71	66.81	90.81	85.78
Forest	98.63	98.53	99.32	93.09	98.53	95.96	98.62	98.13
Water	86.83	100	72.93	100	84.56	100	93.9	90.47
Overall accuracy	86.79		81.25		81.7		85.73	
Kappa	0.85		0.79		0.79		0.84	
classes	**Intensity log**		**Intensity**		**Pottier**		**NN**	
Constructing	88.25	80.03	75.04	74.09	99.68	98.74	96.75	89.99
Industry	68.06	80.77	76.4	75.27	55.62	82.63	61.32	80.21
High Density	74.18	79.02	61.97	78.21	71.52	57.61	68.02	67.90
Low Density	73.8	64.12	66.11	59.69	74.52	56.52	77.76	64.77
Park	46.13	87.57	27.81	80.67	15.51	70.25	41.62	87.66
Pasture	88.95	78.78	88.74	72.21	76.35	68.07	85.98	63.55
Golf Course	82.97	68.65	77.82	68.85	60.43	52.49	77.76	74.02
Street	62.47	49.27	62.45	49.41	55.23	46.81	62.47	47.80
Wide Road	56.16	36.49	59.84	37.69	68.39	33.38	68.39	40.83
Crop 1	97.06	92.08	97.11	91.01	90.66	99.76	90.38	87.14
Crop 2	88.74	95.57	84.57	88.11	91.55	80.21	98.42	91.69
Crop 3	93.09	85.84	85.21	77.82	62.52	82.46	85.25	99.88
Forest	99.2	97.89	98.65	94.31	92.94	87.74	97.85	98.45
Water	87.82	99.98	84.56	94.44	74.31	53.96	84.50	100
Overall accuracy	84.28		80.67		75.56		82.13	
Kappa	0.82		0.78		0.72		0.80	

References

[1] Ban, Y., H. Hu and I. Rangel., 2010. Fusion of QuickBird MS and RADARSAT SAR data for urban land-cover mapping: object-based and knowledge-based approach. Int. J. Remote Sens., Vol.31(6), pp.1391-1410

[2] Angelos Tzotsos., 2006. A support vector machine approach for object based image analysis. 1st International Conference on Object-based Image Analysis. Proc. OBIA.

[3] H. Hu and Ban, Y., 2008. Urban landuse/land-cover mapping with high-resolution SAR imagery by integrating support vector machines into object-based analysis. Proc. SPIE, Vol. 7110.

[4] Pal, M. and Mather, P. M., 2005. Support vector machines for classification in remote sensing. Int. J. Remote Sens., Vol.26 (5), pp.1007–1011.

[5] Cloude, S.R. and Pottier, E., 1997. Application of the H/A/alpha polarimetric decomposition theorem for land classification. Proc. SPIE, Vol. 3120, pp.132-143.

[6] Cloude, S.R. and Pottier, E., 1996. A review of target decomposition theorems in radar polarimetry. IEEE Trans. Geoscience and Remote Sensing (GRS), Vol. 34(2), pp. 498–518.

[7] Definiens Imaging, eCognition user guide, URL: http://www.definiens-imaging.com

[8] Rignot E, Chellappa R Dubois P., 1992. Unsupervised segmentation of polarimetric SAR data using the covariance matrix. IEEE Trans. Geoscience and Remote Sensing, Vol. 30, pp.697—705.

[9] Lukin, V., Ponomarenko, N., Kurekin, A., Lever, K., Pogrebnyak, O., and Sanchez-Fernandez, L., 2006.Approaches to Classification of Multichannel Images. Proc. CIAPR, pp.794-803

[10] Lee, J. S., 1981. Refined filtering of images using local statistics. Computer Graphics and Image Processing, Vol.15, pp.380-389.

[11] Baatz, M. and Schäpe, A., 2000. Multiresolution segmentation - an optimization approach for high quality multi-scale image segmentation, Proc. Angewandte Geographische Informationsverarbeitung XII, Beiträge zum AGIT-Symposium Salzburg 2000, pp.12-23.

[12] Muller, K.-R., Mika, S., Ratsch, G., Tsuda, K., and Scholkopf, B., 2001. An introduction to kernel-based learning algorithms," IEEE Trans. Neural Networks, Vol.12 (2), pp.181-201.

[13] Hsu, C.W. and Lin, C.J., 2002. A Comparison of Methods for Multiclass Support Vector Machines. IEEE Trans. Neural Networks, Vol.13 (2), pp.415-425.

[14] Chang, C.-C. and Lin, C.-J., "LIBSVM: A library for support vector machines, " URL: http://www.csie.ntu.edu.tw/~cjlin/libsvm/

[15] Griffiths, P., Hostert, P., Gruebner, O. and van der Linden, S., 2010. Mapping megacity growth with multi-sensor data. Remote Sensing of Environment, Vol.114 (2), pp.426-439.